



---

**Título artículo / Títol article:** Characterization of silica–water nanofluids dispersed with an ultrasound probe: A study of their physical properties and stability

**Autores / Autors** Rosa Mondragón Cazorla,  
José Enrique Juliá Bolívar,  
Antonio Barba Juan,  
Juan Carlos Jarque Fonfría

**Revista:** Powder Technology Volume 224, July 2012

**Versión / Versió:** Pre-print

**Cita bibliográfica / Cita bibliogràfica (ISO 690):** MONDRAGÓN CAZORLA, Rosa, JULIÁ BOLÍVAR, José Enrique, BARBA JUAN, Antonio, JARQUE FONFRÍA, Juan Carlos. Characterization of silica–water nanofluids dispersed with an ultrasound probe: A study of their physical properties and stability. *Powder Technology*, 2012, Vol. 224.

**url Repositori UJI:** <http://hdl.handle.net/10234/69180>

# **Characterization of silica-water nanofluids dispersed with an ultrasound probe: a study of their physical properties and stability**

Rosa Mondragon<sup>1</sup>, J. Enrique Julia<sup>2</sup>, Antonio Barba<sup>1</sup>, Juan Carlos Jarque<sup>1,\*</sup>

<sup>1</sup> Instituto de Tecnología Cerámica. Universitat Jaume I.  
Campus de Riu Sec. 12071-Castellón de la Plana. Spain

<sup>2</sup> Departamento de Ingeniería Mecánica y Construcción. Universitat Jaume I  
Campus de Riu Sec. 12071-Castellón de la Plana. Spain

\* Corresponding author. E-mail: [juancarlos.jarque@itc.uji.es](mailto:juancarlos.jarque@itc.uji.es). Tel: +34 964 34 24 24

## **Abstract**

The stability and agglomeration state of nanofluids are key parameters for their use in different applications. Silica nanofluids were prepared by dispersing the nanoparticles in distilled water using an ultrasonic probe, which has proved to be the most effective system and gives the best results when compared with previous works. Results were obtained concerning the influence of the solid content,  $pH$  and salt concentration on the zeta potential, electrical double layer, viscosity, elastic and viscous moduli, particle size and light backscattering. Measurement of all these properties provides information about the colloidal state of nanofluids. The most important variable is the solid content. Despite the agglomeration due to high concentration, nanofluids with low viscosity and behaving like liquid were prepared at 20% of mass load thanks to the good dispersion achieved with the ultrasonic treatment. The  $pH$  of the medium can be used to control the stability, since the nanofluids are more stable under basic conditions far from the isoelectric point (IEP) and settle at  $pH = 2$ . Therefore, stable nanofluids for at least 48 h, with high solid content, can be prepared at high  $pH$  value ( $pH > 7$ ) due to the electrostatic repulsion between particles.

**Key words:** suspensions, nanoparticles, dispersion, properties, stability

## 1. Introduction

Aqueous suspensions of particles with particle size in the 5-nm to about the 100-nm range are of great interest in many applications due to their high stability, for example in paints, dyes, ceramics and coatings. These suspensions (called “nanofluids” for the first time by Choi [1] to refer to fluids with suspended nanoparticles) can remain for very prolonged periods of time without significant settling or loss of stability [2]. Stability in colloid science is used not only in the thermodynamic sense but also in a strictly colloidal sense. “Colloidally stable” means that the colloidal particles do not settle and do not agglomerate at a significant rate.

The dispersion of dry particles in liquids has been the most frequently used method to produce nanofluids (two-step method) [3, 4]. To make stable dispersions it is necessary to disperse the large agglomerates that form the initial dry powder into primary particles. The equipment used to disperse nanoparticles includes ultrasonic bath [5-9], ultrasonic probe [10-12], magnetic stirrer, high-shear mixer [13], homogenizer and ball mill. Both the processing time and the energy influence the dispersion effect. It has been demonstrated that the ultrasonic probe is the most effective dispersion system due to its higher energy density that breaks the agglomerates more easily than the other mechanisms [11, 14, 15]. Only 2-4 minutes (depending on the conditions of the nanofluid) are needed to obtain well-dispersed suspensions.

After dispersion, primary nanoparticles have a tendency to re-agglomerate due to the nature of the forces present among them. The classical DLVO theory predicts the stability of the nanofluids by knowing the total energy of interaction between two particles [2, 16-18]. In the range of sizes of nanofluids, the ratio *particle surface* to *particle volume* is so high that all the interactions are controlled by short-range forces like Van der Waals attraction and surface forces. When nanoparticles come into contact due to their Brownian motion, they will remain together as a consequence of the Van der Waals attractive force unless a longer-range repulsive force acts to prevent particles from approaching each other. The classical theory only takes into account the electrostatic repulsion [19]. Steric repulsion forces and repulsive solvation forces may be also present in the system [20].

In aqueous media, interparticle interactions at a given concentration can be changed by varying the ionic strength and the *pH* of the suspension [17, 18]. Electrostatic repulsion is preferred for these systems. Knowing the influence that each

of the above-mentioned variables has on the interactions makes it possible to predict the stability and the behaviour of nanofluids prepared under different conditions.

When solids are suspended in water, the surface charge acquired depends on the  $pH$  of the medium. For each system and chemical substance there is a  $pH$  value at which the surface charge in the shear plane that surrounds the particle takes a value of zero. This  $pH$  is known as isoelectric point (IEP) [19]. Consequently, to prepare well-stabilized suspensions,  $pH$  values far away from the isoelectric point are needed.

For the particular system of silica, some authors [2, 6, 7, 9] have noticed an abnormal stability at low  $pH$  values near the isoelectric point, which contrasts with that predicted by the classical DLVO theory. This means that there exists another repulsive short-range force that is not considered in the theory. This force appears as a consequence of the hydration of the particles due to the capacity of silanol groups to form hydrogen bonds with water. This hydration layer acts as a steric mechanism of repulsion.

Regarding the influence of ionic strength, when the particle surface is charged, it is modified by the presence of electrolytes. As a result of the introduction of the electrolyte, the counterions are distributed around the particles and form an electrical double layer consisting of an inner layer (where the counterions are adsorbed) and a diffuse layer (formed by weakly-bounded ions).

The length of the electrical double layer,  $\kappa^{-1}$  (the Debye length), decreases as the ionic strength increases due to the high concentration of ions adsorbed on the particle surface and the compression of the layer. Electrolytes have a screening effect, i.e. the counterions offset the surface charges, thus decreasing the electrostatic repulsion.

With regard to the influence of solid content, the arrangement of the particles in the system depends on the volume occupied in relation to the total volume. For low solid contents, the distances among the particles are high compared to their radius and they can move freely, driven by the Brownian motion. On increasing the solid content, the hydrodynamic interactions as well as the probability of collision become important, thereby enhancing the aggregation processes. At these concentrations the movement of the particles is constricted by the neighbour particles.

The rheological behaviour and the physical properties of nanofluids are directly related to the agglomeration state of the particles, and therefore depend on the variables

that modify their total interaction potential:  $pH$  and electrolyte concentration. Measurement of all the properties of nanofluids allows their stability to be determined and, moreover, the conditions that provide suspensions with suitable characteristics for each application can be established.

## **2. Survey of previous work**

The dispersion, stability and physical properties of silica nanofluids have been studied previously by other authors under different experimental conditions. In those works different Aerosil powders suspended in water were studied. Aerosil powders are commercial fumed silicas provided by Degussa in dry powder. Different sorts of Aerosil are available with different particle size.

Table 1 summarizes the variables studied in each work, the different properties measured and the dispersion system used to prepare the nanofluids. The main results obtained are also shown.

From previous works it can be seen how the final properties of nanofluids depend on the characteristics of the suspension and the dispersion process. Different results have been obtained in each work but all of them achieve high viscosities and gel formation when increasing the solid content even for values that are not particularly high. All nanofluids were prepared by means of low energy systems (ultrasonic bath, minishaker, high shear mixer) and some of them do not control all the variables. This means that a better dispersion can be achieved with a correct dispersion system and with a good control of the properties that influence dispersion and stability.

In this work, an ultrasonic probe of high energy density was used to disperse the nanoparticles. The influence of the nanofluid characteristics ( $pH$ , solid content and salt content) on all the properties that give information about the stability and particle agglomeration (zeta potential, Debye length, viscosity, elastic modulus, viscous modulus, particle/agglomerate size, the light backscattering and the backscattering variation rate) was studied. As a result, a complete characterization of well-dispersed nanofluids was obtained and the conditions required to prepare nanofluids with different agglomeration states for further applications were also established.

### 3 Experimental techniques

The following sections offer a description of the experimental techniques used to measure all the properties of the nanofluids that were analysed in order to obtain information about the agglomeration state and the stability of the suspensions. All the tests were carried out at 25 °C.

#### Zeta potential, $\psi$

The zeta potential was measured using a Zetasizer Nano ZS (Malvern Instruments Ltd., UK) from the electrophoretic mobility of particles when an electric field is applied. This velocity is measured using Laser Doppler Velocimetry (LDV) and the zeta potential is obtained through the Henry equation [7].

#### Debye length, $\kappa^{-1}$

The following equation can be used to link the thickness of the electrical double layer and the ionic strength for a symmetrical electrolyte in aqueous solution:

$$\kappa^{-1} = 0.215 \cdot 10^{-9} \cdot \sqrt{I}$$

where  $I$  is the ionic strength of the medium, which is calculated from the electrical conductivity. Griffin and Jurinak [22] obtained the following empirical equation to calculate the ionic strength in suspensions in which sodium and chloride ions are present:

$$I = 0.013 \cdot EC$$

where  $EC$  is the electrical conductivity of the suspension, which was measured directly using an EC-Meter Basic 30+ conductimeter (Crison Instruments S.A., Spain).

#### Viscosity, $\eta$

The viscosity and rheological behaviour of nanofluids were obtained by conducting tests under steady state conditions using a Bohlin CVO-120 rheometer (Malvern Instruments Ltd., UK). A double gap (DG 40/50) device composed of two concentric cylinders suitable for low viscosity suspensions was used. In the gap between the inner cylinder (diameter = 40 mm) and the outer cylinder (diameter = 50 mm) the sample is introduced. A cylindrical device with diameter of 45.46 mm is submerged into the sample creating the double gap. Before each test, a pre-treatment, in which the

samples are submitted to a constant shear stress, was applied to the nanofluids for 30 seconds to ensure similar starting conditions for all them.

#### Elastic modulus and viscous modulus, $G'$ , $G''$

The elastic modulus and viscous modulus (also known as storage and loss moduli, respectively) were obtained by conducting tests under dynamic oscillatory conditions using a Bohlin CVO-120 rheometer (Malvern Instruments Ltd., UK). A cone/plate (CP4°/40) device composed of a flat plate and a cone was used. First, strain sweep tests were carried out at a constant frequency in order to establish the linear viscoelastic region in which the strain does not influence the value of the modules. Finally, frequency sweep tests at a constant strain were performed.

#### Particle size, $d_p$

The particle size distributions were determined by dynamic light scattering (DLS) using a Zetasizer nano ZS (Malvern Instruments Ltd., UK). Particle size was measured from the velocity of the particles due to their Brownian motion by means of the Einstein-Stokes equation.

#### Light backscattering, $BS$

The amount of light backscattered by the nanofluid from an incident laser beam was measured using a Turbiscan Lab Expert (Formulaction SA, France). Measurements are based on the multiple light scattering theory. This equipment consists of a pulsed near-infrared light source and a detector that measures the light backscattered by the sample. For each nanofluid, the backscattering profiles were obtained along the height cell. To analyse the stability of nanofluids the measurements were carried out at different time intervals up to a total time of 48 hours.

## **4 Materials**

All the experiments were carried out with silica nanofluids. Commercial colloidal silicas are commonly available in the form of sols or powders. One particular form of silica powder of interest is fumed silica. Fumed silica produced by flame hydrolysis of chlorosilane ( $\text{SiCl}_4$ ) is the most hydrophilic silica and an extremely versatile material which also has unique properties [9].

In this work, commercial fumed silica provided by Degussa was used. Specifically, the silica chosen was an Aerosil 200 consisting in amorphous hydrophilic



silica nanoparticles with primary units of 12 nm and a density of 2200 kg/m<sup>3</sup> according to the manufacturer.

The nanoparticles were acquired in dry powder form and were observed by means of scattering electron microscopy. It can be seen in Figure 1 a) that almost all the nanoparticles are in agglomerate form with a larger size than the primary particles. Therefore, when dispersing them with water, it is very important to break the agglomerates down into the primary nanoparticles or into micro-agglomerates of the defined size. In Figure 1 b) the primary particles are shown.

#### ***4.1 Characterization of nanoparticles***

Initially, the nanoparticles were characterized in terms of their specific surface and isoelectric point.

The specific surface was measured using a TriStar 3000 instrument (Micromeritics Instrument Corporation, USA). This equipment determines the specific surface of powder samples by adsorption of nitrogen gas using the BET method.

Experimental results yield a value of  $211 \pm 7$  m<sup>2</sup>/g for the specific surface. This value is in good agreement with the specific surface provided by the manufacturer, which has a value of  $200 \pm 25$  m<sup>2</sup>/g.

The isoelectric point was obtained from the zeta potential curves. The zeta potential represents the electrostatic potential of the particles and is proportional to their surface charge. The isoelectric point is the *pH* value at which the surface charge and the zeta potential take a value of zero. To determine the isoelectric point of the silica nanofluids, the zeta potential of suspensions prepared under different conditions of *pH* and salt concentration was measured. All the measurements were carried out in dilute suspension.

Figure 2 shows the variation of zeta potential with *pH* and salt concentration. The *pH* of the nanofluid was modified by adding HCl or NaOH solutions. It can be seen that the isoelectric point corresponds approximately to *pH* = 2. When the *pH* is increased above this value, particles acquire a negative charge and the zeta potential increases negatively. The origin of the surface charge is the ionisation of reactive silanol groups (-SiOH). At *pH* levels above the isoelectric point, the neutral silanol groups adsorb hydroxyl groups and the particles become negatively charged, while at *pH*

values lower than the isoelectric point, the free protonated water reacts with silanol groups and forms positive groups.

The screening effect of the salt can also be seen. An increase in the salt concentration leads to a decrease in the surface charge and the zeta potential due to the selective adsorption of ions on the particle surface that counteracts the particle charge.

#### ***4.2 Preparation of nanofluids***

Nanofluids with different particle concentrations were prepared by adding distilled water containing different concentration of NaCl salt to the defined amounts of nanoparticles. In this method, known as the two-step method, the nanoparticles are purchased as dry powder and then dispersed in the liquid medium. The solid content is expressed in terms of mass fraction (w/w) which represents the weight of solid respect to the weight of the suspension.

Of all the dispersion methods available, dispersion with ultrasonic probes has been confirmed as the most effective one. Therefore, in this work dispersion was performed using an ultrasonic probe (UP400s from Hielscher Ultrasonics GmbH, Germany). Initially, the mixture of nanoparticles with the water or the salt solution was submitted to a sonication treatment for a period of time. After that, the *pH* of the nanofluid was modified by adding HCl or NaOH solutions (0.01 w/w). The quantities added to the nanofluids are so small that they are negligible and do not affect the total volume. Finally, to ensure correct dispersion of all the components, the nanofluids are submitted to a second sonication treatment for 2 minutes.

To determine the period of time necessary to disperse the nanoparticles, the influence of the first sonication time on the viscosity was obtained for suspensions at a solid content,  $Y_s$ , of 0.20 w/w,  $pH = 10$  and no salt addition. These conditions provide the highest viscosity before the ultrasonic treatment and make the time obtained to reduce the viscosity suitable for the rest of suspensions. Figure 3 shows the evolution of the viscosity at different shear rates with the total sonication time, taking into account both the first sonication time and the 2-minute treatment performed after *pH* adjustment. It can be seen that even for the worst condition at high solid content, after 5 minutes (3 + 2 minutes) the viscosity does not change significantly. Moreover, the differences in viscosity depending on the shear rate for a constant time are negligible after 5 minutes.

That means that the rheological behaviour is less shear-thinning and the dispersion is better. Therefore, this was the time chosen to carry out all the tests.

## **5 Results and discussion**

### **5.1 Experimental matrix**

To analyse the effect of the variables that influence the aggregation state and stability of nanofluids, a Design of Experiments (DoE) based on the Taguchi orthogonal arrays was chosen [23, 24].

The three input variables studied were the solid mass load,  $Y_s$ , the  $pH$  of the nanofluid, and the salt concentration,  $[NaCl]$ . The orthogonal array chosen for this case was  $L_9 (3^4)$ , which consists in a three-level design for four input variables arranged in four columns. In this array the single effects of the variables in columns 3 and 4 in it, are confounded with the effect of the interaction of the variables in columns 1 and 2 in the array. In this work only three variables were analysed, so the first column has been eliminated to avoid confusion of effects. A total of nine experimental tests were carried out (Exp 1-9). The first four columns in Table 2 show the experimental conditions of each test. This low number of experiments made it possible to obtain the main single effects and the levels of the variables that optimize the properties of nanofluids.

The seven output variables measured were the zeta potential of nanofluids,  $\psi$ , the Debye-length,  $\kappa^{-1}$ , the viscosity,  $\eta$ , the elastic modulus,  $G'$ , the viscous modulus,  $G''$ , the particle size,  $d_p$ , the initial light backscattering,  $BS$ , and the variation of  $BS$  with time.

### **5.2 Influence of variables on the stability and aggregation state**

Table 2 also shows the results obtained for each of the six output variables measured. Moreover, from the variation in light backscattering with time, a variation rate was obtained with which to study the stability of nanofluids.

All the results were analysed using the ANOVA method and the significance of each single effect on each output variable was obtained. This method determines the degree of significance from the probability of the Fisher distribution. It is said that an input variable has a statistically significant effect on the output variable at the 95% confidence level when the probability of the F-distribution is less than 0.05. Table 3 shows the values obtained for the probability of the F-distribution for each input

variable and measured property. In the sections that follow, all the results and the analysis of variables are shown.

#### Zeta potential, $\psi$

It can be seen in Table 3 that the only variable which can be considered to have a significant effect in the range studied is the  $pH$  of the nanofluid. Figure 4 a) shows how the zeta potential increases in the negative sense when increasing the  $pH$  value. When the  $pH$  is raised above the isoelectric point ( $pH = 2$ ), the surface charge of the nanoparticles is increased and as a result the absolute value of the zeta potential also increases [6, 7, 9, 19].

The global effect of the solid content cannot be considered significant due to the high error bars obtained from the ANOVA method, following the Least Significant Difference procedure, only with the values of the three experiments carried out for each level of the input variable. However, in Figure 4 b) it can be seen how the increase of solid mass load from 0.10 to 0.20 w/w leads to a decrease in the zeta potential and the surface charge. For high solid contents, the particles form agglomerates and the electrophoretic mobility and potential measured correspond to those agglomerates that behave like bigger particles with a lower specific surface area.

#### Debye length, $\kappa^{-1}$

It can be seen in Table 3 that neither the  $pH$  nor the solid content exerts a significant influence on the Debye length. It is shown that the only variable which has a significant effect is the salt concentration, which, as can be observed in Figure 5, has a negative effect. On increasing the salt concentration, the ionic strength of the medium is also increased and the electrical double-layer is compressed, as mentioned before.

#### Viscosity, $\eta$

As a result of the viscosity measurements, the rheograms of each nanofluid were obtained. The rheological behaviour is also used to determine the degree of dispersion of nanofluids [25-27]. When agglomerates are present in the suspension, its behaviour becomes shear-thinning. This means that viscosity is high at low shear rates, but decreases on increasing the shear rate due to the break-up of the agglomerates into the primary particles or stable lower-sized aggregates. In contrast, for well-dispersed nanofluids the behaviour becomes Newtonian and the viscosity is independent of the

shear rate. Figure 6 shows the rheological behaviour of all the nanofluids tested. It can be seen that all the nanofluids prepared at a solid mass load of 0.20 (Exp 1, Exp 4 and Exp 7) present a slightly shear-thinning behaviour due to the increase in the probability of collision among particles, which favours the formation of agglomerates. Moreover, the nanofluids of Exp 6 and Exp 8, which correspond to suspensions with a lower solid content but prepared at  $pH = 2$ , also display this shear-thinning behaviour as a consequence of the zero charge of particles (isoelectric point) and their agglomeration. The rest of the nanofluids present a Newtonian behaviour. From these flow curves it can be concluded that high solid contents and  $pH$  values close to the isoelectric point lead to the agglomeration of particles, as expected.

To analyse the viscosity results by the ANOVA method, discrete values are needed. For the Newtonian nanofluids, the viscosity equals the proportional constant that relates strain stress and shear rate and is obtained from the linear regression. For the shear-thinning nanofluids, the viscosity at low shear rates was used.

It can be seen in Table 3 that neither the  $pH$  nor the salt concentration has statistically significant effects on the viscosity. It is shown that the only variable that has a significant effect in the range of variables studied is the solid content, which has a positive effect, as can be seen in Figure 7. It is known that the viscosity of a suspension increases on adding solid particles due to the hydrodynamic interactions as well as the colloidal interactions that take place in the fluid flow [28-31]. It can be seen that on increasing the solid mass load from 0.02 to 0.10 there is no significant increase, but when raised from 0.10 to 0.20 the viscosity rises significantly due to the increase in the interactions and collisions among particles that lead to the formation of agglomerates.

#### Elastic modulus, $G'$ and viscous modulus, $G''$

The measurements of the viscoelastic behaviour were used to obtain the evolution of each modulus with the oscillation frequency, as can be seen in Figure 8. This behaviour is used to determine whether the nanofluids behave like a liquid with well-dispersed particles or, instead, like a solid with agglomerates that lead to gel formation. It can be observed that for all the nanofluids that were prepared, the viscous modulus is higher than the elastic one. That means that the viscous part is predominant and all the suspensions behave like a liquid. These suspensions follow the viscoelastic liquid model proposed by Maxwell. In this model the elastic modulus is proportional to

the square of the frequency, while the viscous modulus is proportional to the frequency [25].

To analyse the results by the ANOVA method, discrete values of each output variable are needed. In this work the values were taken at a constant frequency of 0.0044 Hz, where there is less variability in the measurements.

For the elastic modulus, it can be observed in Table 3 that no input variable has a significant effect. As mentioned above, all nanofluids behave like a liquid with a very small elastic part and, consequently, this part is negligible and the modulus is independent of the properties of the nanofluid.

For the viscous modulus, it can be concluded that no variable has a significant influence on the viscous modulus. Due to the like liquid behaviour of the nanofluids, the viscous part, although predominant, presents small values and this behaviour is independent of the properties of the nanofluid. For the solid content (Figure 9), although its effect is not statistically significant, the viscosity and hence the viscous part increase with solid content due to the increase in the interaction among particles.

#### Particle size, $d_p$

The particle size distribution of each nanofluid was obtained from Dynamic Light Scattering measurements (Figure 10). The measurements were carried out under the experimental conditions established in Table 2, so the diameters obtained correspond to the size of the particles or agglomerates present in the suspension under those conditions without dilution. As can be seen, the particle size distributions go from monomodal for the dispersed ones to bimodal and trimodal for the agglomerated ones. For nanofluids with high solid contents, the distributions become polymodal due to the presence of secondary agglomerates. These agglomerates are formed as a result of the instability of the system and the high number of interactions, and they cannot be broken down into primary particles.

It can be seen that even in the best-dispersed nanofluid, the particle size is 15 times the primary particle size (12 nm). This means that particles form stable aggregates in aqueous suspension even after the ultrasonic treatment. One of the reasons for this behaviour is the process used to produce nanoparticles [14]. Aerosil 200 is a fumed silica obtained by high-temperature hydrolysis of silicon tetrachloride in a hydrogen/oxygen flame. During the process, primary particles (5-100 nm) are produced

first. These particles collide and sinter, giving rise to fractal aggregates of a larger size (100-500 nm).

To study the formation of agglomerates by the ANOVA method, the mean particle sizes of the biggest agglomerates were analysed. That is to say, the median particle size was taken into account for the monomodal distributions and the median particle size of the highest size mode was used in the case of the polymodal distributions. The primary agglomerates that are not broken down into secondary agglomerates are the ones that give information about the degree of dispersion achieved.

From Table 3 it can be seen that no input variable has an influence on the particle size. However, it is obvious from the previous figure that the solid content really affects the particle size and the shape of the distribution. As in all the other properties studied above, the solid content favours the presence of agglomerates. The problem is that the error bars obtained by the Fisher's Least Significant Difference (LSD) procedure are so big that the differences cannot be considered of significance, as can be seen in Figure 11.

#### Light backscattering, BS and variation rate

The amount of light backscattered by the nanofluid from an incident light depends on the aggregation state of the nanoparticles and the turbidity of the nanofluid. When particles agglomerate, that cluster presents a refractive index that is different from the dispersed particles [16]. The initial backscattering can be used to obtain the degree of dispersion of nanofluids. Moreover, the evolution of the backscattering with time gives information about the stability of the nanofluids and the time they can remain without settling or forming a gel. Figure 12 shows the evolution of light backscattering with time at the bottom of the sample.

First, the initial light backscattering was analysed using the ANOVA method. This initial value is the same at any point in the sample (flat profile). It can be seen in Table 3 that the only variable which can be considered to have a significant effect is the solid content. In Figure 13 it can be observed that the increase in the solid content leads to an increase in the light backscattering, as expected. On increasing the solid content, the agglomerate size increases and the turbidity is also increased. As a result, the amount of light backscattering is higher than the amount of transmitted light. This increase is not constant and solid mass loads from 0.02 to 0.10 are more important as a

result of the change in the particle size distribution. The big change takes place when passing from monomodal (dispersed) to bimodal (agglomerate). Further changes from bimodal to trimodal are not so important because the nanoparticles are agglomerated in any case.

The evolution of backscattering with time at the bottom of the sample was employed to calculate a variation rate for the first hours when the main changes take place. It can be concluded from Table 3 that no variable has a significant effect on the BS variation rate. However, the most important parameter in this case is the  $pH$  of the nanofluid. In Figure 14 it can be seen that for  $pH$  values further away from the isoelectric point where the particles are charged there is no variation in BS with time, while from  $pH = 2$  there exists a higher rate. However, as in the case of the particle size, the error bars obtained by the LSD method are so high that the effect cannot be considered significant.

The effect of the  $pH$  can be also seen in Figure 12. In Exp 1, Exp 6 and Exp 8, all of them at  $pH = 2$  (isoelectric point), the backscattering initially decreases throughout the whole sample due to the increase in the size of the agglomerates (theory of multiple light scattering for particle sizes higher than 0.3 nm). When the size of the agglomerates reaches a certain value, they start to settle. At the bottom of the sample the solid fraction increases and therefore the amount of light backscattered starts to increase. Only for Exp 1 the BS decreases continuously due the higher solid content ( $Y_s = 0.20$  w/w), which makes the agglomerate form, first, a three-dimensional network and finally a gel.

In consequence, although the initial degree of dispersion only depends on the solid content, the stability of the nanofluids with time depends on the  $pH$  of the suspension. At  $pH > 7$ , nanofluids are stable for at least 48 hours independently of the solid content. Figure 15 shows two images of the sample corresponding to Exp 7 ( $Y_s = 0.20$ ,  $pH = 10$ ,  $[NaCl] = 0.01M$ ) just after the ultrasonic treatment and after depositing for 48 h.

## 6 Conclusions

In this work silica nanofluids were prepared using an ultrasonic probe, which has previously been confirmed as the most effective dispersion system. The influence of solid content,  $pH$  and salt concentration on the stability and dispersion of silica



nanofluids was analysed from the measurement of the physical properties that are related to the agglomeration state, i.e. zeta potential, Debye length, viscosity, elastic and viscous moduli, particle size, light backscattering and *BS* variation rate. All nanofluids were fully characterized and all their properties were measured.

As expected, the input variable that presents the greatest influence on the properties of the nanofluid is the *solid content*. Higher amounts of particles lead to a higher number of interactions among them and there is a greater probability of agglomeration. Hence, on increasing the solid content, the viscosity of the nanofluids, the viscous nature, the particle size and the turbidity of the suspension all increase too. However, despite this agglomeration, nanofluids up to 20% w/w with low viscosity (42.80 mPa·s in the worst case), behaving like a liquid ( $G'' > G'$ ) and stable for a minimum of 48 hours, were prepared.

The *pH* of the nanofluid has an important effect on the zeta potential and the stability of the suspensions. The isoelectric point was obtained at  $pH = 2$ . At this value, particles have no surface charge and they agglomerate easily when they approach each other, due to the Brownian motion. For low solid contents, particles agglomerate and settle, while for high solid contents the agglomerates form a three-dimensional network and the nanofluid becomes a gel. At *pH* values a long way away from the isoelectric point, particles acquire a surface charge and electrostatic repulsion controls the system. In these conditions nanofluids are stable for at least 48 hours.

Finally, the *salt concentration*, in the range of the variables analysed, only affects the electrical double layer but not the other properties. It has been stated that for salt concentrations lower than 0.2 M, the ionic strength does not influence the hydration repulsion present in the silica system [7]. Therefore, although the electrical double layer is reduced and the distance at which the electrostatic repulsion is effective decreases, the hydration repulsion remains and counteracts the Van der Waals attraction. As a result, for these low salt concentrations the increase in the ionic strength does not affect the agglomeration state and the final properties.

From the results obtained, the conditions needed to produce stable silica nanofluids at a certain solid content, with low viscosity and like liquid behaviour, consist in a high energy treatment with an ultrasound probe for 5 minutes, basic media (*pH* values higher than 7) and no salt addition.

## Acknowledgments

R. Mondragón thanks the Spanish Ministry of Education for a pre-doctoral fellowship (FPU program, Ref. AP2008-01077).

The authors gratefully acknowledge the financial support from the Spanish Ministry of Science and Innovation (projects CTQ2010-21321-C02-01 and CTQ2010-21321-C02-02).

## References

- [1] U.S. Choi, Enhancing thermal conductivity of fluids with nanoparticles, ASME FED 231 (1995) 99-103.
- [2] H.E. Bergna, W.O. Roberts, Colloidal silica: Fundamentals and applications, CRC Taylor & Francis, 2006.
- [3] D. Wen, Y. Ding, Formulation of nanofluids for natural convective heat transfer applications, Int. J. Heat Fluid Flow 26 (2005) 855-864.
- [4] Y. Li, J. Zhou, S. Tung, E. Schneider, S. Xi, A review on development of nanofluid preparation and characterization, Powder Technology 196 (2009) 89-101.
- [5] M.L. Fisher, M. Colic, M.P. Rao, F.F. Lange, Effect of silica nanoparticles size on the stability of alumina/silica suspensions, J. Am. Ceram. Soc. 84 (2001) 713-718.
- [6] S. Chen, G. Oye, J. Sjöblom, Rheological properties of aqueous silica particle suspensions, J. Disper. Sci. Technol. 26 (2005) 495-501.
- [7] S. Chen, G. Oye, J. Sjöblom, Effect of pH and salt on rheological properties of aerosol suspensions, J. Disper. Sci. Technol. 28 (2007) 845-853.
- [8] J.H. Lee, K.S. Hwang, S.P. Jang, B.H. Lee, J.H. Kim, S.U.S. Choi, C.J. Choi, Effective viscosities and thermal conductivities of aqueous nanofluids containing low volume concentrations of Al<sub>2</sub>O<sub>3</sub> nanoparticles, Int. J. Heat Mass Transfer, 51 (2008) 2651-2656.
- [9] A. Amiri, G. Oye, J. Sjöblom, Influence of pH, high salinity and particle concentration on stability and rheological properties of aqueous suspensions of fumed silica, Colloids and surfaces A: Physicochem. Eng. Aspects, 349 (2009) 43-54.

- [10] U. Paik, J. Yul Kim, V.A. Hackley, Rheological and electrokinetic behaviour associated with concentrated nanosized silica hydrosols, *Mat. Chem. Phys.* 91 (2005) 205-211.
- [11] I. Santacruz, K. Anapoorani, J. Binner, Preparation of high solid content nanozirconia suspensions, *J. Am. Ceram. Soc.* 91 (2008) 398-405.
- [12] S. Fazio, J. Guzman, M.T. Colomer, A. Salomoni, R. Moreno, Colloidal stability of nanosized titania aqueous suspensions, *J. Eur. Ceram. Soc.* 28 (2008) 2171-2176.
- [13] P. Ding, A.W. Pacek, De-agglomeration of silica nanoparticles in the presence of surfactants, *J. Disper. Sci. Technol.* 29 (2008) 593-599.
- [14] G. Petzold, R. Rojas-Reyna, M. Mende, S. Schwarz, Application relevant characterization of aqueous silica nanodispersions, *J. Disper. Sci. Technol.* 30 (2009) 1216-1222.
- [15] M.J. Pastoriza-Gallego, C. Casanova, R. Paramo, B. Barbes, J.L. Legido, M.M. Piñeiro, A study on stability and thermophysical properties (density and viscosity) of Al<sub>2</sub>O<sub>3</sub> in water nanofluid, *J. Appl. Phys.* 106 (2009) 064301.
- [16] R.K. Iler, *The chemistry of silica: solubility, polymerization, colloid and surface properties, and biochemistry*, John Wiley & Sons, 1979.
- [17] D.J. Shaw, *Introduction to colloid and surface chemistry*, Butterworth-Heinemann: Oxford, UK, 1991.
- [18] D. Quemada, C. Berli, Energy of interaction in colloids and its implication in rheological modelling, *Adv. Colloid Interface Sci.* 98 (2002) 51-85.
- [19] R.J. Hunter, *Zeta potential in colloid science. Principles and applications*, Academic Press Limited, 1988.
- [20] S. Song, C. Peng, Thickness of salvation layers on nano-scale silica dispersed in water and ethanol, *J. Disper. Sci. Technol.* 26 (2005) 197-201.
- [21] A.W. Pacek, P. Ding, A.T. Utomo, Effect of energy density, pH and temperature on de-aggregation in nano-particles/water suspensions in high shear mixer, *Powder Technology*, 173 (2007) 203-210.
- [22] G.P. Griffin, J.J. Jurinak, Estimation of activity coefficients from the electrical conductivity of natural aquatic systems and soil extracts, *Soil Sci.* 116 (1973) 26-30.
- [23] G. Taguchi, *System of experimental design*, New York: UNIPUB/Kraus International, 1987.
- [24] H.M. Wadsworth, *Handbook of statistical methods for engineers and scientists*, McGraw-Hill, 1990.

- [25] H.A. Barnes, J.F. Hutton, D.K. Walters, An introduction to rheology, Elsevier, 1989.
- [26] D. Quemada, Rheological modelling of complex fluids. I. The concept of effective volume fraction revised, *Eur. Phys. J. Appl. Phys.* 1 (1998) 119-127.
- [27] J. Chevalier, O. Tillement, F. Ayela, Structure and rheology of SiO<sub>2</sub> nanoparticle suspensions under very high shear rates, *Phys. Rev.* 80 (2009) 051403.
- [28] I.M. Krieger, Rheology of monodisperse lattices, *Adv. Colloid Interface Sci.* 3 (1972) 111-136.
- [29] D. Quemada, Rheology of concentrated disperse systems and minimum energy dissipation principle. I. Viscosity-concentration relationship, *Rheological Acta*, 16 (1977) 82-94.
- [30] C.J. Rueb, Flow properties of a colloidal gel, University of Illinois, PhD Thesis, 1994.
- [31] F.J. Rubio-Hernandez, M.F. Ayucar-Rubio, J.F. Velazquez-Navarro, F.J. Galindo-Rosales, Intrinsic viscosity of SiO<sub>2</sub>, Al<sub>2</sub>O<sub>3</sub> and TiO<sub>2</sub> aqueous suspensions, *J. Colloid Interface Sci.* 298 (2006) 967-972.

## Figure captions

Figure 1. Nanoparticles of Aerosil 200 observed by SEM.

Figure 2. Variation of zeta potential with  $pH$  and salt concentration. Isoelectric point.

Figure 3. Evolution of viscosity with sonication time at different shear rates.

Figure 4. Zeta potential: Influence of a)  $pH$  and b) solid content.

Figure 5. Debye length: Influence of salt concentration.

Figure 6. Rheograms measured from the nanofluids tested.

Figure 7. Viscosity: Influence of solid content.

Figure 8. Viscoelastic behaviour from the nanofluids tested. Solid symbol:  $G'$ ; Hollow symbol:  $G''$

Figure 9. Viscous modulus: Influence of solid content.

Figure 10. Particle size distribution for the nanofluids tested.

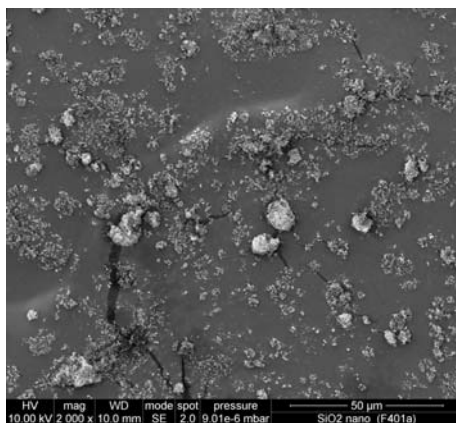
Figure 11. Particle size: Influence of solid content.

Figure 12. Evolution with time of light backscattering at the bottom of the sample.

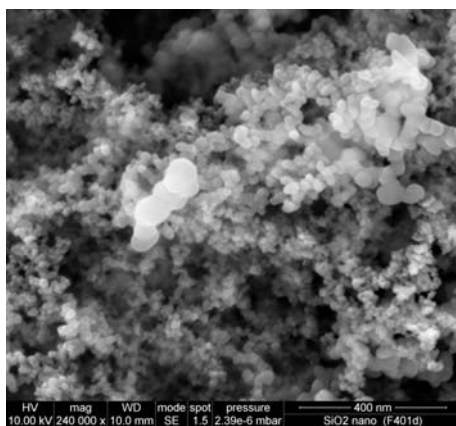
Figure 13. Light backscattering: Influence of solid content.

Figure 14. Backscattering variation rate: Influence of  $pH$ .

Figure 15. Nanofluid at  $Y_S = 0.20$ ,  $pH = 10$  and  $[NaCl] = 0.01M$  a) just after the ultrasonic treatment and b) after depositing for 48 h.



a)



b)

**Figure 1. Nanoparticles of Aerosil 200 observed by SEM.**

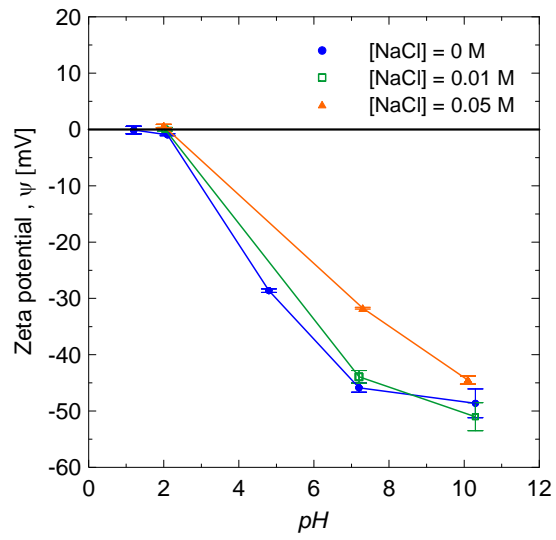


**Figure 2. Variation of zeta potential with *pH* and salt concentration. Isoelectric point.**

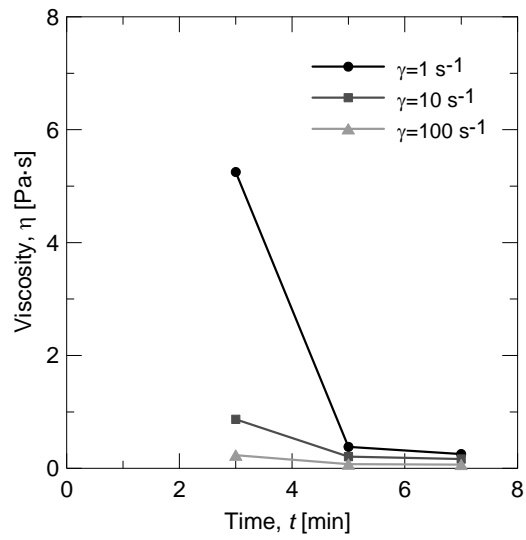
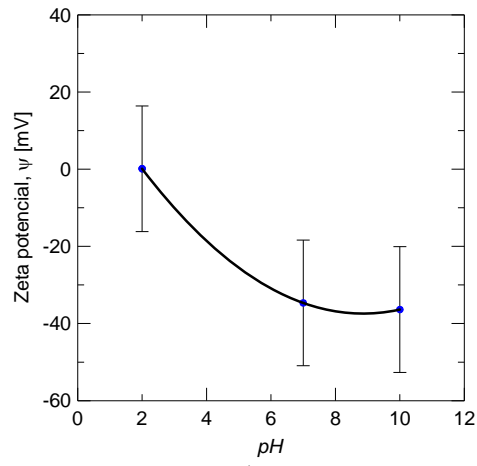
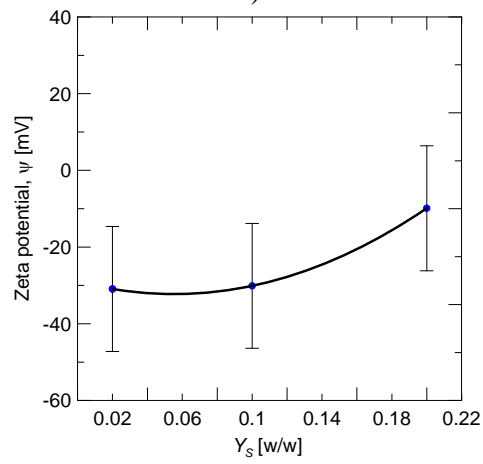


**Figure 3. Evolution of viscosity with sonication time at different shear rates.**





a)



b)

**Figure 4. Zeta potential: Influence of a)  $pH$  and b) solid content.**

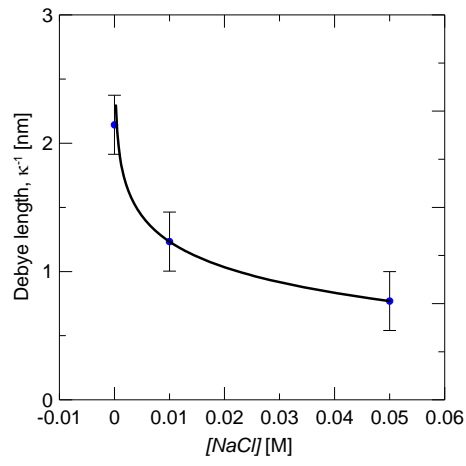


**Figure 5. Debye length: Influence of salt concentration.**

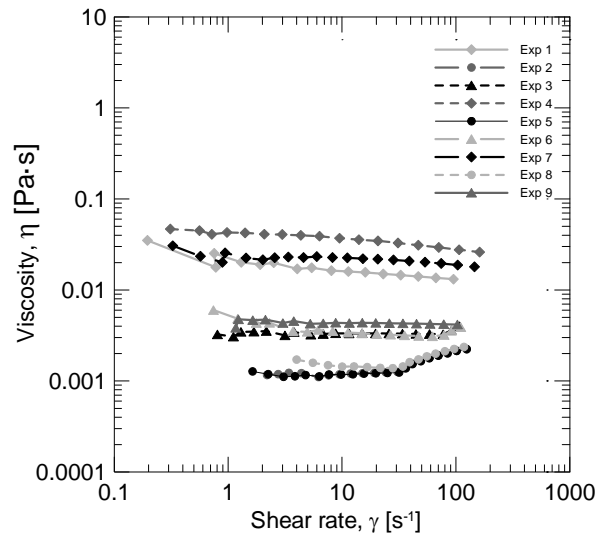


**Figure 6. Rheograms measured from the nanofluids tested.**

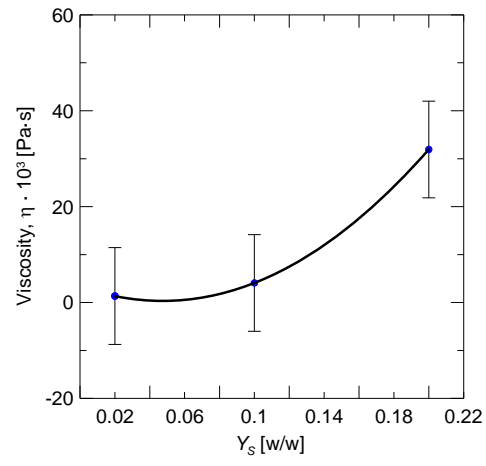


**Figure 7. Viscosity: Influence of solid content.**

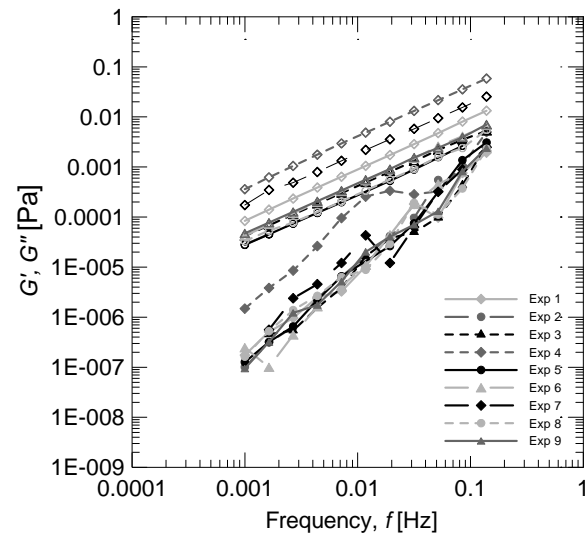


**Figure 8. Viscoelastic behaviour from the nanofluids tested. Solid symbol:  $G'$ ; Hollow symbol:  $G''$**

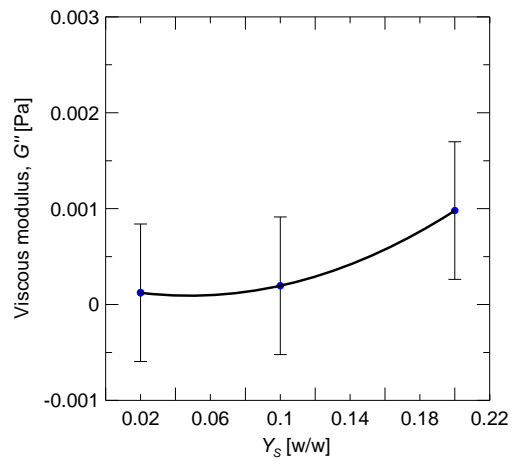


**Figure 9. Viscous modulus: Influence of solid content.**

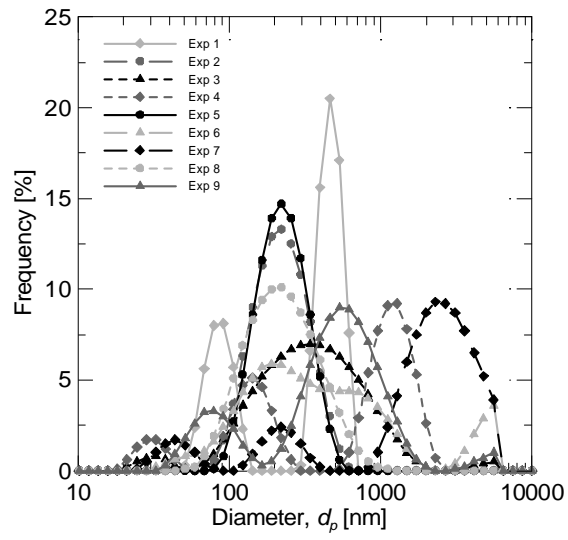


**Figure 10. Particle size distribution for the nanofluids tested.**

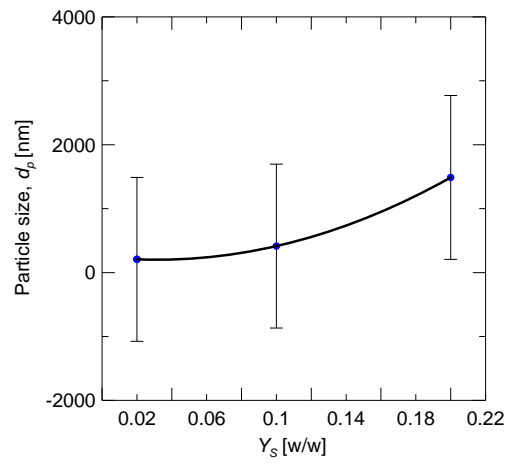


**Figure 11. Particle size: Influence of solid content.**



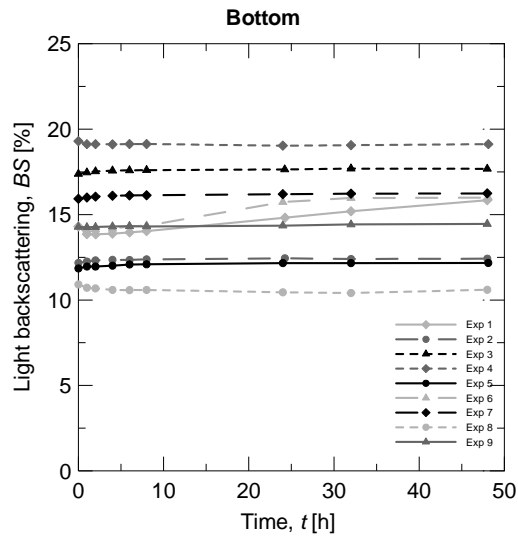
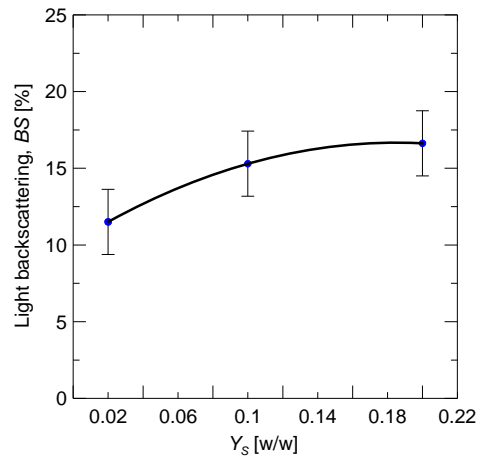
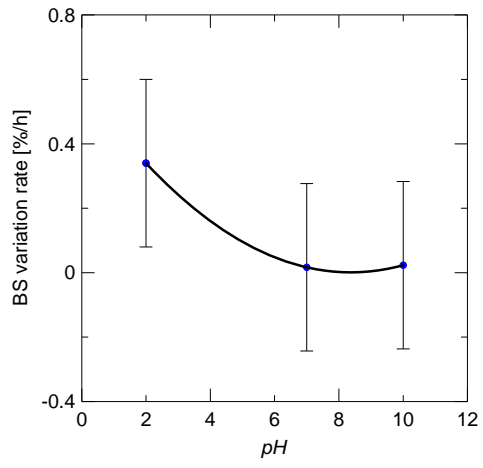


Figure 12. Evolution with time of light backscattering at the bottom of the sample.



**Figure 13. Light backscattering: Influence of solid content.**



**Figure 14. Backscattering variation rate: Influence of *pH*.**



a)

b)

**Figure 15. Nanofluid at  $Y_S = 0.20$ ,  $pH = 10$  and  $[NaCl] = 0.01M$  a) just after the ultrasonic treatment and b) after depositing for 48 h.**

**Table captions**

Table 1. Summary of previous works.

Table 2. Experimental matrix and results.

Table 3. Probability of the F-distribution.

**Table 1. Summary of previous works.**

<b>Ref.</b>	<b>Materials</b>	<b>Variables studied</b>	<b>Measured properties</b>	<b>Dispersion system</b>	<b>Results</b>
Paik et al., 2005 [10]	Aerosil 90	<i>pH</i> , salt concentration	Zeta potential, Viscosity	Ultrasonic treatment	Highest viscosities far from the IEP, contrary to the DLVO theory.
Chen et al., 2005 [6]	Aerosil 200	--	Particle size, viscosity, elastic and viscous moduli	Minishaker and ultrasonic bath	Gel formed at volume fractions higher than 6%. "Like solid" behaviour. <i>pH</i> and salt not controlled.
Chen et al., 2007 [7]	Aerosil 200	<i>pH</i> , salt concentration	Particle size viscosity elastic and viscous moduli	Minishaker and ultrasonic bath	Viscosities up to $10^6$ mPa·s for 0.05 volume fraction. Change from "like liquid" to "like solid" behaviour depending on the <i>pH</i> .
Pacek et al., 2007 [21]	Aerosil 200V	Energy input, <i>pH</i> , temperature	De-agglomeration of particles	High shear mixer	High energy is needed to break secondary agglomerates into primary ones.
Ding and Pacek, 2008 [13]	Aerosil 200V	Surfactants (PVP, SDS, PEG), <i>pH</i>	De-agglomeration of particles	High shear mixer	None of the surfactants used enabled the de-agglomeration of nanopowders.
Amiri et al., 2009 [9]	Aerosil 200	<i>pH</i> , salt concentration	Zeta potential, viscosity, elastic and viscous moduli, light transmission	Minishaker and ultrasonic bath	[NaCl] > 0.6M and volume fraction of 0.023 leads to shear-thinning and like solid behaviour, and yield stress.
Petzold et al., 2009 [14]	Aerosil powders	--	De-agglomeration of particles	Ultrasonic probe, magnetic stirrer, ultraturrax	The ultrasonic probe is the most effective dispersion system due to the high energy applied.

**Table 2. Experimental matrix and results.**

<b>Exp</b>	$Y_s$ [w/w]	$pH$	$[NaCl]$ [M]	$\psi$ [mV]	$\kappa^{-1}$ [nm]	$\eta \cdot 10^3$ [Pa·s]	$G' \cdot 10^6$ [Pa]	$G'' \cdot 10^4$ [Pa]	$d_p$ [nm]	$BS$ [%]	$BS$ <i>Variation</i> [%/h]
1	0.20	2	0	-0.22	2.09	27.43	2.520	3.880	468	14.44	0.60
2	0.02	7	0.01	-44.72	1.49	1.26	2.367	1.233	201	11.90	0.03
3	0.10	10	0.05	-44.50	0.74	3.27	1.542	1.842	381	17.44	0.02
4	0.20	7	0.05	-13.40	0.88	42.8	26.201	17.607	1234	19.43	0.01
5	0.02	10	0	-48.63	2.03	1.24	2.193	1.210	205	11.78	0.02
6	0.10	2	0.01	0.03	1.32	4.82	1.611	1.960	332	14.11	0.32
7	0.20	10	0.01	-16.00	0.89	25.56	4.560	7.922	2762	16.00	0.03
8	0.02	2	0.05	0.59	0.69	1.58	2.664	1.258	216	10.84	0.10
9	0.10	7	0	-45.85	2.31	4.18	1.743	2.075	531	14.34	0.01

**Table 3. Probability of the F-distribution.**

<b>Input variable</b>	$\psi$	$\kappa^{-1}$	$\eta$	$G'$	$G''$	$d_p$	$BS$	<i>BS Variation</i>
$Y_S$	0.1678	0.4305	0.0370	0.4026	0.1976	0.2731	0.0645	0.5198
$pH$	0.0633	0.1642	0.5182	0.4913	0.4963	0.5375	0.2630	0.1761
$[NaCl]$	0.3762	0.0116	0.5546	0.4876	0.508	0.5812	0.2346	0.5125